Photomicrocalorimetry: photosubstitution of carbonyl by phosphites in [Mn(η^5-C$_5$H$_4$CH$_3$)(CO)$_3$]

Palmira B. Dias, Clementina Teixeira, Alberto R. Dias

Centro de Química Estrutural, Instituto Superior Técnico, 1096 Lisboa Codex (Portugal)

José de Alencar Simoni

Instituto de Química, Universidade Estadual de Campinas, 13081 Campinas, S. Paulo (Brazil)

José A. Martinho Simões

Departamento de Química, Faculdade de Ciências, Universidade de Lisboa, 1700 Lisboa (Portugal)
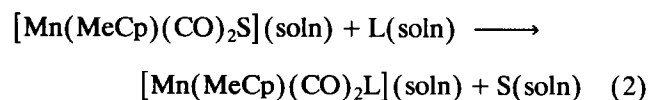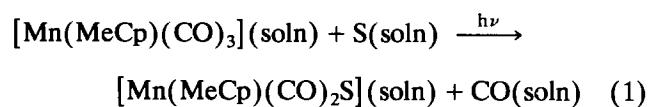
Abstract

A photomicrocalorimeter is described for studies of reactions involving oxygen and moisture-sensitive compounds in organic solvents. This calorimeter was used to investigate the thermochemistry of photochemical substitutions of a carbonyl in [Mn(η^5-C$_5$H$_4$CH$_3$)(CO)$_3$] by P(OR)$_3$ (R = Ph or ^{i}Pr). The measured reaction enthalpies in heptane (λ = 400 nm), ΔH_r = − 15.7 ± 0.5 and − 18.6 ± 0.9 kJ mol^{-1}, respectively, were identified with the bond dissociation enthalpy differences D(Mn–CO) − D[Mn–P(OPh)$_3$] and D(Mn–CO) − D[Mn–P(O^{i}Pr)$_3$] in solution. These results are discussed in terms of the basicity of the phosphites, spectroscopic data of the complexes (CO stretching frequencies), and the available thermochemical data for other transition metal-phosphorus(III) ligand interactions.

Key words: Manganese; Photosubstitution; Photomicrocalorimetry; Bond enthalpies; Phosphite; Thermochemistry

1. Introduction

Despite the importance of transition metal complexes containing phosphorus(III) ligands in many synthetic and catalytic processes [1,2], data on metal–phosphorus bonding energetics are still scarce [3]. In the present paper we report thermochemical observations on reactions involving the replacement of a carbonyl in [Mn(MeCp)(CO)$_3$] (MeCp = η^5-C$_5$H$_4$CH$_3$) by P(OPh)$_3$ or P(O^{i}Pr)$_3$. The complex and its cyclopentadienyl analogue are remarkably inert towards thermal substitution, which hinders the use of classical methods, such as reaction-solution calorimetry, to probe their thermochemistry. However, they undergo efficient photochemical substitutions by almost any nucleophile with very high quantum yields (0.65–1.0) in the near-UV [4,5]. This has been the favourite synthetic method of preparing complexes [Mn(MeCp)(CO)$_2$L] (reactions 1 and 2) [6–11]. The photochemical cleavage of one carbonyl is followed by the coordination of a solvent molecule S (such as diethyl ether, tetrahydrofuran and alkanes), yielding [Mn(MeCp)(CO)$_2$S] This species then reacts with the nucleophile (L), giving [Mn(MeCp)(CO)$_2$L] (L = pyridine, amine, phosphines, phosphites, thiols, *etc.*).

$$[\text{Mn(MeCp)(CO)}_3](\text{soln}) + \text{S(soln)} \xrightarrow{h\nu}$$

$$[\text{Mn(MeCp)(CO)}_2\text{S}](\text{soln}) + \text{CO(soln)} \quad (1)$$

$$[\text{Mn(MeCp)(CO)}_2\text{S}](\text{soln}) + \text{L(soln)} \longrightarrow$$

$$[\text{Mn(MeCp)(CO)}_2\text{L}](\text{soln}) + \text{S(soln)} \quad (2)$$

These reactions are well documented in the literature and under controlled conditions are clean processes [4]. For the analogous cyclopentadienyl complex,

[Mn(Cp)(CO)₃], photoacoustic calorimetry experiments afforded the enthalpy of reaction 1 (S = heptane) and the enthalpies of reaction 2 for several L (thf, acetone, cis-cyclooctene, dibutylsulphide, haloalkanes, and silanes) [6–8].

We have used photomicrocalorimetry [12] to measure the enthalpy of reaction 3 in heptane solution for L = P(OPh)₃ or P(OⁱPr)₃, and to derive the bond dissociation enthalpy differences D(Mn–CO) – D(Mn–L).

$$[Mn(MeCp)(CO)_3](\text{soln}) + L(\text{soln}) \xrightarrow{h\nu}$$

$$[Mn(MeCp)(CO)_2L](\text{soln}) + CO(\text{soln}). \quad (3)$$
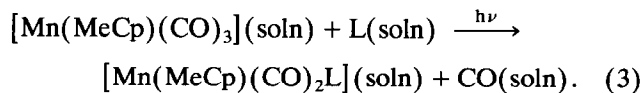
Photocalorimetry can be attractive for the study of the thermochemistry of reactions in solution, particularly when those reactions are not amenable to calorimetric methods based on thermal activation. It has been used to investigate a variety of light-induced processes in several areas [12], including transition metal coordination chemistry [13–16], organic chemistry [17,18], polymer science [19–22], biochemistry [23–27], and biology [28,29]. As suggested by its name, photocalorimetry relies on standard calorimetric equipment, usually an isoperibol or a heat-flux calorimeter, coupled with optical devices that allow the irradiation of the sample contained in the reaction vessel. The instrument used in the present work is a microcalorimeter of the heat-conduction type, allowing the use of very small and dilute samples. As described below, the light is led into the sample cell through several optical fibres.

The basis of photocalorimetry is rather simple. Light of energy E_p, supplied to the calorimetric vessel filled with a photoinert reference or blank, is quantitatively transformed into heat, Q', and this quantity is measured. In another run, the same amount of energy is used to activate the photosensitive substance and a reaction occurs. The difference between Q' and the heat recorded in this second run, Q, enables one to derive the enthalpy associated with the photochemical reaction, ΔH_r, if the molar conversion of the reactant (n) is known (eqn. 4):

$$\Delta H_r = \frac{Q' - Q}{n} \quad (4)$$

2. Experimental section

2.1. Photomicrocalorimetry

The photomicrocalorimeter (Fig. 1) is a modified version of the instrument developed by Teixeira and Wadsö [30] and was briefly described in previous reports [12,17,31]. Only one of the four twin heat-conduction microcalorimeters of the Thermal Activity
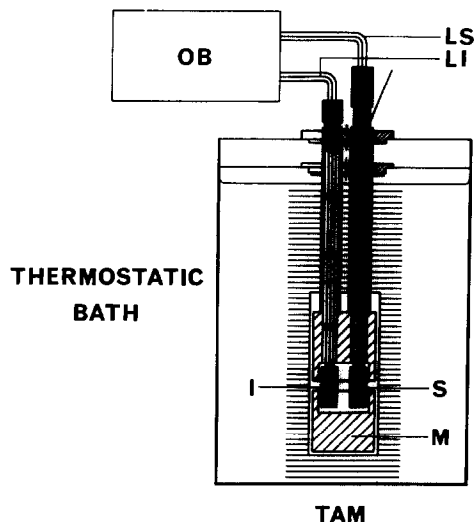

TAM

Fig. 1. One channel version of the photomicrocalorimeter. OB — optical bench; M — heat conduction twin microcalorimetric unit or channel; I — photoinert light absorption vessel; S — photochemical vessel; LI and LS — optical cables to vessels I and S.

Monitor (TAM) from ThermoMetric, Sweden (5 ml ampoule channel 2277-201) [32] was required for the type of measurement made in the present study. Each channel or microcalorimeter is an independent differential unit, sharing with the others a thermostatic bath with a stability of $\pm 1 \times 10^{-4}$ K over extended periods (in our case the mean temperature was set to 298.15 K). A modular system of insertion vessels with different geometries can be fitted into each channel, in opposition to each other [31,33]. In a typical experiment, the base line is first recorded for this twin system at thermal equilibrium. When a physical or chemical process occurs in the main vessel, the heat exchange with the surroundings is detected as a power output which is amplified and recorded as a function of time. This signal can be computer integrated and the total amount of heat determined by electrical or chemical calibration.

The vessels S and I (Figs. 1 and 2) used in this work were described in detail elsewhere [30]. However, as illustrated in Fig. 2, several modifications were made in both vessels in order to use organic solvents (heptane and decane have been tested) under an inert atmosphere. The main photochemical vessel S is a modified version of the prototype of the perfusion/titration cell from ThermoMetric 2277-402 [33], adapted with three optical plastic cables (Mitsubishi, Japan) and an injection titration tube [30]. In order to prevent any leak of the solvent, the following changes were made to the lid (Fig. 2B): the titration tube, which was not used in these experiments, was replaced by a Teflon plug; the steel sleeves (2 mm o.d.), to which the optical fibres (1
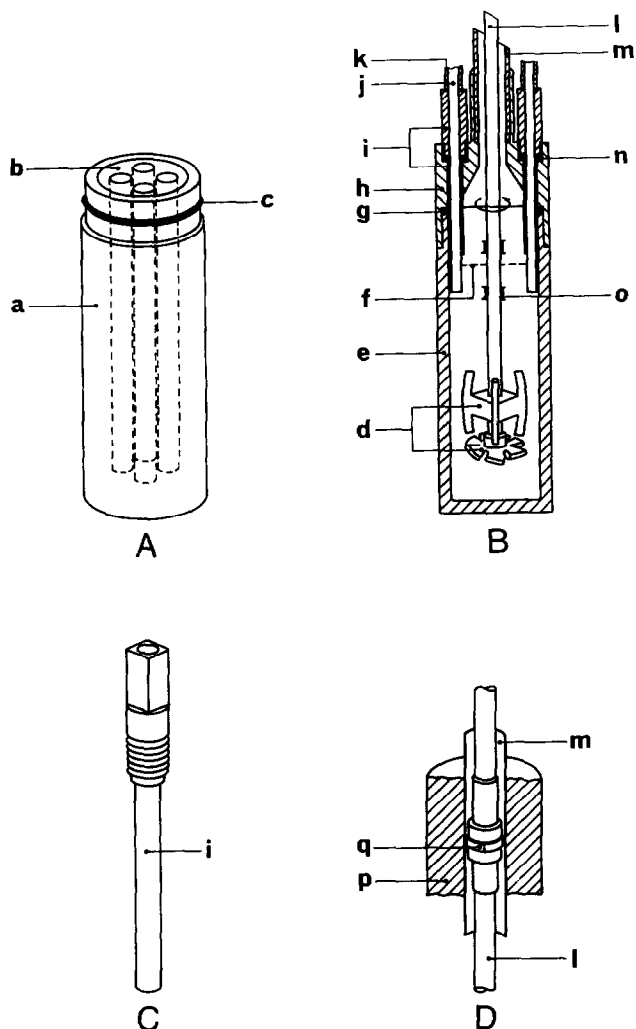
Fig. 2. Modifications of the photomicrocalorimetric assembly for studies with organic solvents. (A) — Details of the absorption compartment of the reference vessel I. a, steel container; b, brass bolt with holes for insertion of the fibres; c, O-ring. (B) — Detail of the photocalorimetric vessel S. d, Teflon stirrers; e, 3 ml stainless steel sample compartment; f, liquid level; g, Teflon sealing ring; h, lid; i, steel sleeve; j, optical fibre, k, plastic protection of the fibre; l, stirrer shaft; m, steel tube; n, Teflon O-ring; o, Teflon "moisturizers". (C) — Detail of the steel sleeve of the fibres (i); the quartz window and Teflon protection jacket are not seen in this Figure (see text). (D) — Detail of the stirring shaft (l). p, brass bolt; q, Teflon O-ring.

mm o.d.) were fixed with epoxy resin after stripped of their plastic sheaths, are longer than in the early version and are screwed to the lid, a tight seal being ensured by a Teflon O-ring. In some experiments a 2 mm diameter quartz window was glued to the end of each sleeve and positioned with the help of a Teflon tube (not shown in Fig. 2), to avoid the contact of the optical fibres with chemically aggressive solutions. In other experiments, a glass or quartz tube was inserted and glued to the sleeve as a protection jacket. How-

ever, as these modifications decrease the amount of light that reaches the sample, they should be used only when necessary. If the chemical attack is very slow, an alternative is simply to cut the tips of the fibres after several experiments. This has been done, for example, in the experiments involving heptane solutions of the manganese complexes, described below.

Teflon "moisturizers" (Fig. 2B) were used to wet the stirring shaft below the Teflon O-ring with the solvent used in the experiment, in order to decrease the time to reach thermal equilibrium. As this Teflon O-ring does not make a tight seal, the water column normally used in the shaft [33] was eliminated. An advantage of the previous change is that it increases the volume to be filled with argon. Both the titration shaft and the 3 ml sample container can be coated with black Teflon for experiments with acid solutions [30]. This coating cannot be used with heptane solutions as it gives rather long equilibration periods. Finally, the cell S can be loaded inside a small glove box, under argon.

The photoinert vessel I transforms light quantitatively into heat. It is a steel ampoule with a brass filling, with four holes for fibre insertion (up to four cables). It was found that the brass filling improves the response of the twin system when the main vessel S was filled with heptane solutions. For water solutions better performance was achieved with the early "steel only" design [30]. Small Teflon plugs can be used to block the holes when a reduced number of fibres is used.

The optical bench (Fig. 3) was modified to maximize the photon fluxes and to compensate partially for the small irradiation area of the fibres ($< 3 \times 1$ mm^2). Most components are from PTI (Photon Technology International). Light from a 100 W tungsten halogen
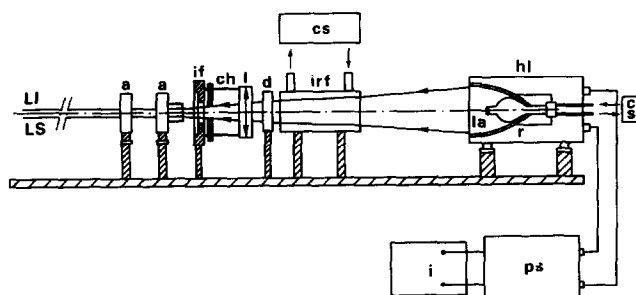

Fig. 3. Optical bench. LS and LI optical cables to vessels S and I; a, slit and adapters; if, linear interference filter Schott Veril BL 200; ch, metallic chopper; l, quartz lens (f = 3.5 cm); d, A001 PTI optical diffuser or homogenizer; irf, A002 PTI stainless steel IR water filter; hl, A1010PTI housing lamp with elliptical reflector r (f = 4.5); la, lamp; ps, power supply PTI LPS-220 with igniter i; cs, automatic water cooling device.

lamp (Flecta or Osram) installed in a housing with an elliptical reflector is IR filtered and homogenized, further focussed with a convergent quartz lens (focal length 3.5 cm), and filtered to about 30 nm band pass by using a 3 mm slit and a linear interference filter (400–1000 nm range). Depending on the energy requirements, this slit can be increased to 1 cm, corresponding to a band pass of *ca.* 45 nm. Several adapters were used for firm mounting of the six optical cables at the focus of the light beam, three for each of the vessels S and I. The fibres were held vertically, at the centre of the slit (other geometries are possible, depending on the filter used). The housing lamp and the IR filter are refrigerated with water from an automatic cooling device, preventing overheating in case of water supply failure. The power supply to the lamp, together with an igniter (Fig. 3), can also power mercury, xenon or mercury-xenon are lamps fitted in the same housing. In the case of the tungsten lamps used in the present work, very stable radiant powers can be supplied to the photomicrocalorimeter, over long periods: for 0.3–1 cm slits and wavelength of *ca.* 436 nm the maximum power can vary from 80 to 190 μW (3×10^{-10} to 7×10^{-10} Einstein s^{-1}) and is stable to within 0.3 μW. The power produced with the early optical bench [30] was below 60 μW, for a band pass of 14 nm, selected with a monochromator and without the use of the elliptical reflector. The comparison indicates that only by increasing the number of optical fibres will it be possible to increase photon flux (a 20 ml photochemical vessel with more fibres is under development) [34].

In the earlier design of the photomicrocalorimeter two calorimetric twin units (or two channels) were used [30]. The present mode of operation, with only one twin unit, requires equal illumination of vessels S and I during the irradiation. This was achieved by adjusting the position of the fibers LS and LI at the beginning of each set of experiments, after loading the vessel S with the solvent. Light was then quantitatively transformed into heat on both sides of the twin system, cancelling the power signals (*i.e.*, the same Q' is measured in both sides). The suppression of the light (or heat) background, enables recording at higher sensitivity. This is illustrated in Fig. 4A.

After the fibres had been adjusted as described in the previous paragraph, the base line remained constant for the periods with and without irradiation. Ideally, no base line shift should be noticed when the light is switched on or off. However, the shadowed areas in Fig. 4A clearly indicate non-steady situations, which arise from the different time constants of the two vessels I and S. As mentioned before, this effect was minimized for the experiments involving heptane by using the cell I with a brass filling.
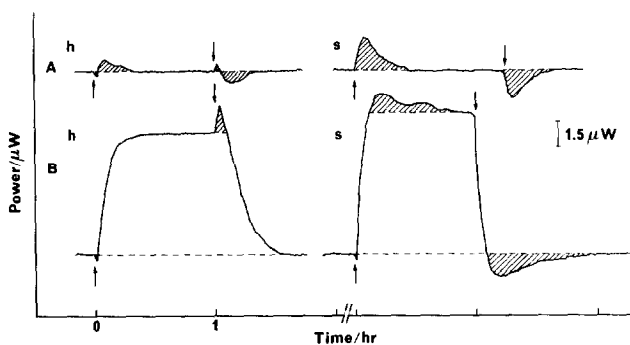

Fig. 4. Typical power *vs.* time records for "one channel operation". A — base line adjustments of the twin system: h, heptane at 400 nm; s, 0.05 M sulphuric acid at 436 nm. B — plots for the photochemical reactions: h, reaction 3 for L = P(OPh)$_3$ at 400 nm; s, reaction 5 at 436 nm. Both processes are exothermic. The arrows indicate the exact moment for switching the light on and off. The shadowed areas indicate nonsteady periods (see text).

After charging the vessel S with the photosensitive compound, without changing the optical geometry, the irradiation begins and the net power signal is recorded as illustrated in Fig. 4B for reactions 3 and 5. The integrated area multiplied by the electrical calibration enables direct calculation of the enthalpy of the reaction using eqn. (4). Note that in the one channel mode of operation E_p is not known, and therefore quantum yield determinations are not possible [12,30], chemical analyses being required to obtain ΔH_r.

Fluctuations of light intensity with time are largely compensated for by the present one channel arrangement, as long as the focus position is not changed. Frequent checks of the base line were made, in order to confirm that the geometry of the optical system had not changed between runs. Fortunately, errors due to small base line shifts or to light intensity fluctuations are not serious, as long as the molar conversion is kept above 10^{-7} mol h^{-1}, preferably ten times as much. Changes in the shape of the tungsten filament, which may cause a shift in the base line, can be reduced by a diffuser (Fig. 3). However, this device leads to a decrease of about 30% in the photon flux.

2.2. Compounds

Potassium tris(oxalato)ferrate(III) K$_3$[Fe(C$_2$O$_4$)$_3$] · 3H$_2$O was prepared as described in the literature [30,35–37]. The actinometer solutions used in the calorimeter and the solutions for dosage of Fe^{II} were made from deionized water saturated with nitrogen. The analytical procedure is described elsewhere [30,35–37].

P(O^{i}Pr)$_3$ (Aldrich) was dried with sodium and distilled under vacuum. P(OPh)$_3$ (Merck) was purified as described in the literature [38].

[Mn(MeCpXCO)$_3$] (Aldrich) was vacuum distilled in the dark and kept under argon prior to use. The complexes [Mn(MeCpXCO)$_2$P(OPh)$_3$] and [Mn(MeCpXCO)$_2$P(O^{i}Pr)$_3$] were prepared as described in the literature [11], with minor modifications. Yellow crystals of the triphenylphosphite complex were obtained from hot hexane solutions. The purification of the trisisopropyphosphite complex was made according to a literature procedure [39]. The purities were checked by elemental analysis and IR spectroscopy.

2.3. Experimental procedure

Additional details of the photocalorimetric experiments were as follows. All the runs involving the tris(oxalato)ferrate(III) and manganese complexes were performed under a dim red light. The solutions of the tricarbonyl-manganese complex with an excess of each phosphite were degassed and vessel S was loaded under argon in a glove box. Dinitrogen was not used because it diffuses faster than argon from the vessel, and also to avoid the formation of a (dinitrogen) manganese complex [40].

The base line adjustments for irradiations at 400 nm (~ 45 nm band pass) are illustrated in Fig. 4. They were checked with ferrocene solutions in heptane, to guarantee that no light losses occur by reflection (ferrocene is photoinert at that wavelength).

The number of moles of reacted tricarbonylmanganese complex, n_{Mn}, was determined spectrophotometrically (Perkin Elmer Lambda 15) by using the relation $\Delta C = \Delta A/l\Delta\epsilon_m$, where ΔC is the decrease in molar concentration of the starting complex, ΔA the difference in absorbance before and after irradiation, $\Delta\epsilon_m$ the difference in the molar extinction coefficients between the parent and the final complex, and l the optical path (0.2 or 0.5 cm). $\Delta\epsilon_m = \epsilon_f - \epsilon_i$ was determined from Lambert-Beer plots for the tricarbonyl and the phosphite complexes at three different wavelengths (Table 1). The IR spectra of the final solutions demonstrated (based on the stretching frequencies of the carbonyl group) [11] that only the monosubstituted complexes [Mn(MeCpXCO)$_2$P(OR)$_3$](R = Ph or ^{i}Pr) were formed.

TABLE 1. Molar extinction coefficients, ϵ_m, for the heptane solutions of the manganese complexes [a]

Complex	310 nm	320 nm	340 nm
[Mn(MeCpXCO)$_3$]	267	356	372
[Mn(MeCpXCO)$_2$P(O^{i}Pr)$_3$]	496	649	853
[Mn(MeCpXCO)$_2$P(OPh)$_3$]	666	894	1103

[a] Values for the tricarbonyl complex are ϵ_i and for the remaining are ϵ_f (see text).

The base line stability with heptane is the same as for water solutions, ± 0.3 μW over 24 hours. All experiments were performed at a stirring rate of 1.5 Hz using a 6920B Meter Calibrator from Hewlett Packard as power supply. The friction from the stirrers produced about 0.8 μW.

Electrical calibrations of vessel S charged with 2.7 ml of deionized MilliPore water were performed as described elsewhere [17,30]. The calibration constant (ϵ) for the manganese systems and for the azobenzene test reaction was $(8.637 \pm 0.055) \times 10^{-4}$ J cm^{-2} (sensitivity 30 μW). In the case of the potassium tris(oxalato)ferrate(III) test reaction, electrical calibration was made using the TAM resistors at the bottom of the channel and led to $\epsilon = (8.857 \pm 0.016) \times 10^{-4}$ J cm^{-2} (sensitivity 30 μW). In the latter experiments the Teflon-coated vessel S was filled with 2.7 ml of 0.05 M H$_2$SO$_4$.

3. Results and discussion

3.1. Test reactions

A good chemical calibration reaction for photocalorimetry should be provided by a photochemical reaction of high quantum yield in the full UV-Vis range and with an accurate and large ΔH_r determined by other experimental technique. To our knowledge, no chemical calibration has been recommended for photocalorimetry. However, several groups have determined the enthalpy of reaction 5, the reduction of Parker's actinometer potassium tris(oxalato)ferrate(III) in 0.05 M H$_2$SO$_4$ [13,23,30], and the results agree within the uncertainty intervals (see below). Reaction 5 was thus used in the present work to assess the performance of our photocalorimeter.

$$[Fe(C_2O_4)_3]^{3-} (soln) \xrightarrow{h\nu}$$
$$[Fe(C_2O_4)_2]^{2-} (soln) + CO_2(soln)$$
$$+ 1/2C_2O_4^{2-}(soln) \quad (5)$$
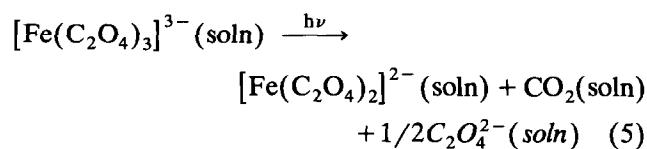
Details of the experimental method were previously reported [30] and the results of the present one channel set-up are shown in Table 2 [41*]. The power vs. time curves for the optical adjustment and the reaction are illustrated in Fig. 4. The value obtained for the enthalpy of reaction 5, $\Delta H_r = -51.2 \pm 2.0$ kJ mol^{-1}, is in good agreement with those published in the literature: $\Delta H_r = -52.6 \pm 0.8$ kJ mol^{-1} (the same method but using two channels) [30]; $\Delta H_r = -53.6 \pm 2.9$ kJ mol^{-1} (irradiation at 446 nm) [13]; $\Delta H_r = -54.0 \pm 8.0$ kJ mol^{-1} [23]. The larger uncertainty of the result reported in the present paper, compared to the value

---

* Reference with asterisk indicates a note in the list of references.

TABLE 2. Photomicrocalorimetric results for the Hatchard-Parker actinometer $K_3[Fe(C_2O_4)_3]\cdot 3H_2O$ (Eq. 5) at 436 nm [a]

$n_{Fe^{II}} \times 10^7$/mol	$(Q'-Q)\times 10^3$/J	ΔH_r/kJ mol^{-1}
7.630	-38.98	-51.08
6.391	-35.67	-55.77
7.658	-39.42	-51.48
6.901	-34.79	-50.42
6.845	-34.35	-50.19
6.171	-29.95	-48.53
	average	-51.2±2.0

[a] Irradiation time 1 h; molar extinction coefficient for the Fe^{II}-phenanthroline complex at 510 nm, $\epsilon_m = 1.114 \times 10^4$ M^{-1} cm^{-1} [30,35-37]. Amplifier sensitivity 30 μW.

in ref. 30, may be due to propagated errors caused by small shifts in the base line between experiments, during the irradiation (possibly due to changes in the position of the fibres at the focus region).

As reported elsewhere [17], the performance of the photomicrocalorimeter with the optical extension described in Fig. 3 was also tested with reaction 6, the isomerization of *trans*- to *cis*-azobenzene in heptane, at 436 nm (bandpass 30-45 nm).

$$\textit{trans}\text{-PhN=NPh(soln)} \xrightarrow{h\nu} \textit{cis}\text{-PhN=NPh(soln)} \quad (6)$$
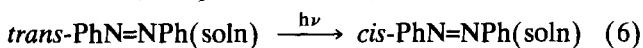
$$\Delta H_r = 48.9 \pm 2.3 \text{ kJ mol}^{-1}$$

Reaction 6 is not wavelength dependent, as proved by the agreement with the value published by Adamson et al., $\Delta H_r = 49.0 \pm 5.4$ kJ mol^{-1} [13], measured with an isoperibol reaction-solution photocalorimeter at 546 nm, in heptane. The value $\Delta H_r = 48.9 \pm 2.3$ kJ mol^{-1}, coupled to the enthalpies of solution of the two isomers in heptane, leads to $\Delta H_r(\textit{trans} \to \textit{cis},$ cr$) = 45.2 \pm 2.4$ kJ mol^{-1}, which is slightly lower than the one obtained by reaction-solution calorimetry data, $\Delta H_r(\textit{trans} \to \textit{cis},$ cr$) = 49.1 \pm 1.0$ kJ mol^{-1} [17]. This small discrepancy, together with the difficulties in handling the solutions in the photomicrocalorimeter (slow attack on the plastic fibres, difficulties in purifying the two isomers, *etc.*), raises questions about the use of azobenzene as a calibration standard for photocalorimetry.

3.2. Manganese complexes

The results for the enthalpies of reaction 3 for $L = P(O^iPr)_3$ and $P(OPh)_3$, are shown in Tables 3 and 4, respectively. An example of a typical power *vs.* time curve is illustrated in Fig. 4.

The average reaction enthalpies in Tables 3 and 4, -18.6 ± 0.9 kJ mol^{-1} and -15.7 ± 0.5 kJ mol^{-1}, can be identified with the *solution values* for the bond dissociation enthalpy differences $D(Mn-CO) - D[Mn-P(O^iPr)_3]$ and $D(Mn-CO) - D[Mn-P(OPh)_3]$, respectively. If it is assumed that the solvation en-

TABLE 3. Calorimetric results for the reaction of $[Mn(MeCp)(CO)_3]$ with $P(O^iPr)_3$ in heptane (reaction 3, $\lambda = 400$ nm) [a]

$n_{Mn} \times 10^6$/mol	t_{irr}/h	$(Q'-Q)\times 10^3$/J	ΔH_r/kJ mol^{-1}
2.09	1.50	-38.50	-18.42
1.74	1.00	-30.72	-17.62
1.32	1.13	-26.82	-20.26
1.83	2.58	-33.09	-18.08
2.46	1.18	-46.25	-18.80
		average	-18.6±0.9

[a] All the experiments were run at 30 μW, with solutions of identical composition: $[Mn(MeCp)(CO)_3] = 4.2 \times 10^{-3}$ M; $n_P / n_{Mn} = 8.8$.

thalpies of products and reactants in reaction 3 are similar [42], then the above ΔH_r results also represent the bond dissociation enthalpy differences in the gas phase. Bearing in mind that the cone angles of both $P(O^iPr)_3$ and $P(OPh)_3$ are similar (130° and 128°, respectively [3]), the fact that $D[Mn-P(O^iPr)_3]$ is slightly larger than $D[Mn-P(OPh)_3]$ (by 2.9 ± 1.0 kJ mol^{-1}) is in keeping with the more basic character of this (isopropyl) phosphite. The pK_a of protonated $P(O^iPr)_3$ is 4.08 as compared with -2.0 for protonated $P(OPh)_3$ [3]. The stronger σ interaction in the case of the alkyl phosphite is also shown by the values of the parameters $^{FT}\chi$, 19.05 and 30.20 cm^{-1}, respectively, for $P(O^iPr)_3$ and $P(OPh)_3$. These $^{FT}\chi$ values have been tabulated by Bartik and coworkers [3,43] and their difference $(-11.15$ cm$^{-1})$ reflects approximately the difference between the carbonyl stretching frequencies in the two complexes [44*].

To our knowledge, other than the thermochemical results reported above, there is no information on the energetics of bonds between manganese (or any other Group 7 metal) and phosphorus(III) ligands. However, the differences $D(Mn-CO) - D[Mn-P(OR)_3]$ can be compared with data derived by photoacoustic calorimetry for the replacement of a carbonyl group in the

TABLE 4. Calorimetric results for the reaction of $[Mn(MeCp)(CO)_3]$ with $P(OPh)_3$ in heptane (reaction 3, $\lambda = 400$ nm) [a]

Solution	$n_{Mn} \times 10^6$ /mol	t_{irr}/h	$(Q'-Q)$ $\times 10^3$/J	ΔH_r/kJ mol^{-1}
A	1.98	2.17	-31.3	-15.81
B	2.30	1.67	-37.7	-16.40
C	2.10	2.41	-33.8	-16.08
D	2.52	1.33	-37.5	-14.88
D	2.17	1.17	-33.5	-15.46
			average	-15.7±0.5

[a] Composition of solutions: $[Mn(MeCp)(CO)_3]$ 1.8×10^{-2} M (A), 2.6×10^{-2} M (B), 5.2×10^{-3} M (C), and 1.8×10^{-2} M (D); the ligand/metal molar ratios, n_P / n_{Mn}, were 10 (A), 11 (B), 12 (C), and 9 (D). The amplifier sensitivity was 30 μW (A, B and D) and 100 μW (C).

TABLE 5. Differences between manganese–carbonyl and manganese–ligand bond dissociation enthalpies in [Mn(MeCp)(CO)$_2$L] and [Mn(Cp)(CO)$_2$L]

L	D(Mn–CO)– D(Mn–L)/kJ mol^{-1}
P(O^{i}Pr)$_3$ [a]	−18.6± 0.9
P(OPh)$_3$ [a]	−15.7± 0.5
Bu$_2$S [b]	69.4±10.9
Et$_3$SiH [b]	111.3±12.4
THF [b]	125.9± 7.7
Me$_2$CO [b]	127.2± 8.2
CH$_2$Cl$_2$ [b]	157.7± 6.2

[a] [Mn(MeCp)(CO)$_2$L]. This work.
[b] [Mn(Cp)(CO)$_2$L]. Refs. 6–8.

complex [Mn(Cp)(CO)$_3$] by several donors [6–8] (Table 5). As expected, Mn–P(OR)$_3$ bond dissociation enthalpies are considerably higher than the bond dissociation enthalpies between manganese and weaker donor molecules such as THF, acetone, halo-alkanes, and silanes.

Bond dissociation enthalpy differences D(M–CO) − D[M–P(OR)$_3$] for other transition metals are also not abundant [3]. Reaction-solution calorimetry results of Hoff and coworkers [3,45,46] show that the solution (THF) values of the mean bond dissociation enthalpy differences between $\overline{D}$(Mo–CO) in Mo(CO)$_6$ [47*] and $\overline{D}$[Mo–P(OPh)$_3$] in the complexes Mo(CO)$_3$ [P(OPh)$_3$]$_3$ and cis-Mo(CO)$_4$[P(OPh)$_3$]$_2$ are close to zero (4 and 2 kJ mol^{-1}, respectively). They also found that the replacement of a carbonyl group in [Mo(Cp)(CO)$_3$H] by P(OMe)$_3$ in THF is exothermic by 19.3 kJ mol^{-1} [48]. This value suggests that the replacement of CO in [Mo(Cp)(CO)$_3$H] by P(OPh)$_3$ will be exothermic 6 kJ mol^{-1} bearing in mind that the experimental data for the differences $\overline{D}$[Mo–P(OMe)$_3$] − $\overline{D}$[Mo–P(OPh)$_3$] are ca. 13 kJ mol^{-1} [3,45,46,49].

A final comment is related to the application of fibre optics in a photocalorimeter. In contrast to other methods of irradiation, involving glass or quartz windows, the fibres do not require substantial modification of the base calorimetric set-up, which can therefore be used for other purposes. However, optical fibres provide a rather small irradiation area, making the alignment of the optical bench more critical and affording low photon fluxes. For these reasons, the conversions are very low (10^{-6} mol h^{-1} is a desirable rate, 10^{-7} mol h^{-1} the minimum) and usually only relatively high quantum yield (> 0.1) processes can be investigated. This may be compensated for by the high sensitivity of the microcalorimeter, but very careful manipulation is then required to reduce other possible sources of error. As mentioned above, the fibres can also interact with the reaction medium and they must be protected if necessary. Attack on the fibres is sometimes revealed

by slow exothermic effects and base line displacements after irradiation. Finally, another advantage of fibre optics over windows is that they decrease any energy losses by reflection and transmission [12].

The use of high-sensitivity heat-conduction microcalorimeters is an advantage over isoperibolic (quasi-adiabatic) calorimeters [12]. Reactions involving optically dense compounds can be monitored for long periods (more than one day) in very dilute samples ($> 10^{-4}$ M), avoiding side reactions and secondary photolysis. However, optical densities should be kept to ca. 1 or 1.5 to guarantee full absorption of light.

Acknowledgments

References and notes

1 J.P. Coleman, L.S. Hegedus, J.R. Norton and R.G. Finke, *Principles and Applications of Organotransition Metal Chemistry*, University Science Books, Mill Valley, 1987, and references cited therein.
2 C.A. McAuliffe, *Comprehensive Coordination Chemistry*, Pergamon, London, 1987, Vol. 2.
3 P.B. Dias, M.E. Minas da Piedade and J.A. Martinho Simões, *Coord. Chem. Rev.*, in press.
4 P.J. Giordano and M.S. Wrighton, *Inorg. Chem.*, 16 (1977) 160.
5 G. Teixeira, T. Avilez, A.R. Dias and F. Pina, *J. Organomet. Chem.*, 353 (1988) 83.
6 J.K. Klassen, M. Selke, A.A. Sorensen and G.K. Yang, *J. Am. Chem. Soc.*, 112 (1990) 1267.
7 P.F. Yang and G.K. Yang, *J. Am. Chem. Soc.*, 114 (1992) 6937.
8 D.M. Hester, J. Sun, A.W. Harper and G.K. Yang, *J. Am. Chem. Soc.*, 114 (1992) 5234.
9 W. Strohmeier, C. Barbeau and D. Von Hobe, *Chem. Ber.*, 96 (1963) 3254.
10 W. Strohmeier, *Angew. Chem.*, 76 (1964) 873.
11 J.W. Hershberger and J.K. Kochi, *Polyhedron*, 2 (1983) 929.
12 C. Teixeira and I. Wadsö, *Netsu Sokutei 21*, (1994) 29.
13 A.W. Adamson, A. Vogler, H. Kunkely and R. Wachter, *J. Am. Chem. Soc.*, 100 (1978) 1298.
14 M. Nakashima and A.W. Adamson, *J. Phys. Chem.*, 86 (1982) 2905.
15 Y. Harel and A.W. Adamson, *J. Phys. Chem.*, 90 (1986) 6690.
16 Y. Harel and A.W. Adamson, *J. Phys. Chem.*, 90 (1986) 6693.
17 A.R. Dias, M.E. Minas da Piedade, J.A. Simoni, J.A. Martinho Simões, C. Teixeira, Y. Meng-Yan, G. Pilcher and H. Diogo, *J. Chem. Thermodyn.*, 24 (1992) 439.
18 Y. Harel, A.W. Adamson, C. Kutal, P.A. Grutsch, and K. Yasufuku, *J. Phys. Chem.*, 91 (1987) 901.

19 E. Theweleit and W. Kunze, *Kunstoffe, 77* (1987) 870.

20 B.K. Appelt and M.J.M. Abadie, *Polym. Eng. Sci., 25* (1985) 935.

21 M.J.M. Abadie and B.K. Appelt, *Bull. Soc. Chim. Fr.,* (1988) 20.

22 H.-J. Timmpe, B. Strehmel, F.H. Roch and K. Fritzsche, *Acta Polymerica, 38* (1987) 238.

23 A. Cooper and C.A. Converse, *Biochemistry, 15* (1976) 2970.

24 A. Cooper, *Methods in Enzymology, 88* (1982) 667.

25 A. Cooper, *Nature, 282* (1979) 531.

26 A. Cooper, S.F. Dixon and M. Tsuda, *Eur. Biophys. J., 13* (1986) 195.

27 N. Langerman, *Methods in Enzymology, LVII* (1978) 540.

28 J.L. Magee, T.W. DeWitt, E.C. Smith, and F. Daniels, *J. Am. Chem. Soc., 61* (1939) 3529.

29 P. McIlvaine and N. Langerman, *Biophys. J., 17* (1977) 17.

30 C. Teixeira and I. Wadsö, *J. Chem. Thermodyn., 22* (1990) 703.

31 P. Bäckman, M. Bastos, L.-E. Briggner, S. Hägg, D. Hallén, P. Lönnbro, S.-O. Nilsson, G. Olofsson, A. Schön, J. Suurkuusk, C. Teixeira and I. Wadsö, *Pure Appl. Chem. 66,* (1994) 375.

32 J. Suurkuusk and I. Wadsö, *Chem. Scripta, 20* (1982) 155.

33 N.M. Görman, J. Laynez, A. Schön, J. Suurkuusk and I. Wadsö, *J. Biochem. Biophys. Methods, 10* (1984) 187.

34 P. Johansson, C. Teixeira, and I. Wadsö, unpublished results.

35 H.J. Kuhn, S.E. Braslavsky and R. Schmidt, *Pure Appl. Chem., 61,* (1989) 187.

36 C.G. Hatchard and C.A. Parker, *Proc. Roy. Soc. London, A235* (1956) 518.

37 J.F. Rebek, *Experimental Methods in Photochemistry and Photophysics,* Wiley, New York, 944, 1982.

38 D.D. Perrin, W.L.F. Armarego, and D.R. Perrin, *Purification of Laboratory Chemicals (2nd ed.),* Pergamon, Oxford, 1980.

39 N.G. Connelly and M.D. Kitchen, *J. Chem. Soc., Dalton Trans.,* (1977), 931.

40 B. Bayerl, K. Schmidt, and M. Wahren, *Z. Chem., 15* (1975) 277.

41 The optical bench was different from the one previously described, a home-made version with similar components but without the elliptical reflector. A 1 cm slit was used (band pass ~ 45 Nm). A Perkin-Elmer Lambda 15 UV-Vis spectrophotometer was used to determine $n_{Fe^{II}}$. The calibration was made as recommended [30,35–37].

42 J.A. Martinho Simões and J.L. Beauchamp, *Chem. Rev. 90* (1990) 629.

43 T. Bartik, T. Himmler, H.-G. Schulte and K. Seevogel, *J. Organomet. Chem., 272* (1984) 29.

44 The experimentally observed CO stretching frequencies are (cm^{-1}): [Mn(MeCp)(CO)$_3$](2024, 1938); [Mn(MeCp)(CO)$_2$P(OPh)$_3$] (1970, 1910); [Mn(MeCp)(CO)$_2$P(OPr)$_3$] (1938, 1876).

45 S.P. Nolan and C.D. Hoff, *J. Organomet. Chem., 290* (1985) 365.

46 S.L. Mukerjee, S.P. Nolan, C.D. Hoff and R. López de la Vega, *Inorg. Chem., 27* (1988) 81.

47 The Mo–CO mean bond dissociation enthalpy used for comparison with $\overline{D}$[Mo–P(OPh)$_3$] in [Mo(CO)$_3${P(OPh)$_3$}$_3$] is the average value of the enthalpy associated to the cleavage of the first three CO groups in molybdenum hexacarbonyl. In the comparison involving cis-[Mo(CO)$_4$ {P(OPh)$_3$}$_2$], $\overline{D}$(Mo–CO) is the average of the enthalpy required to cleave the first two CO groups in Mo(CO)$_6$ See Ref. 3.

48 S.P. Nolan, R. Lopez de la Vega, S.L. Mukerjee and C.D. Hoff, *Inorg. Chem., 25* (1986) 1160.

49 S.L. Mukerjee, R.F. Lang, T. Ju, G. Kiss, C.D. Hoff and S.P. Nolan, *Inorg. Chem., 31* (1992) 4885.